OSBP-related protein 4L (ORP4L) interacts with the phosphoinositide 5-phosphatase OCRL1

PRO GRADU

Saundarya Shah

A thesis submitted in confirmatory with the requirements for the degree of Master of Science

Faculty of Biological and Environmental Sciences

University of Helsinki

Tiedekunta – Fakultet – Faculty	Koulutusohjelma – Utbildingsprogram – Degree Programme
Biological and Environmental sciences	Master's Degree Programme in Biotechnology (MBIOT)

Tekijä – Författare – Author

Saundarya Shah

Työn nimi – Arbetets titel – Title

OSBP-related protein 4L (ORP4L) interacts with the phosphoinositide 5-phosphatase OCRL1

Oppiaine/Opintosuunta – Läroämne/Studieinriktning – Subject/Study track

Biotechnology

Työn laji – Arbetets art – Level	Aika – Datum – Month and year	Sivumäärä – Sidoantal – Number of pages
MSc thesis	May, 2019	38

Tiivistelmä – Referat – Abstract

OCRL1 is a phosphatase that cleaves phosphatidylinositol 4,5-bisphosphate (PI4,5P) to phosphatidylinositol-4-phosphate (PI4P). ORP4 is a lipid binding/transport protein implicated in G-protein coupled signaling, cellular calcium homeostasis, proliferation and viability. OCRL1 and ORP4 are found in the endoplasmic reticulum and membrane contact sites throughout the endosomal system and the Golgi complex. OCRL1 is also present in the plasma membrane and vesicular structures. ORP4 has high affinity for binding sterols through the OSBP related domain (ORD). ORP4 also interacts with vimentin intermediate filaments via the ORD and influences the localization and organization of vimentin. The membrane lipid phosphatidylinositol (PI) can be phosphorylated either singly or in combination at three different positions on its inositol ring (D-3, D-4, and D-5)—yielding 8 possible phosphoinositides; the interconversion between the species is regulated by kinases and phosphatases that either add or remove phosphate groups from the various positions on the ring. Phosphoinositide metabolism is heavily involved in signal transduction pathways and cytoskeletal organization. Interestingly, it has also been found to be spatially regulated with distinct phosphoinositides being enriched in particular membrane compartments. BiFC assays can provide an important tool for visualizing protein-protein interactions. Not only is BiFC able to determine protein-protein proximity but it is also able to localize the interaction with regard to compartment membranes and structures. This study examined the interaction of ORP4 with OCRL1 by using BiFC analysis. We were able to determine that the protein pair seems to be in close proximity in the endoplasmic reticulum near the Golgi. Interaction only took place when the OCRL1 was tagged with VB at the C-terminal.

Avainsanat – Nyckelord – Keywords

PIP,OCRL;OSBP,ORP4

Ohjaaja tai ohjaajat – Handledare – Supervisor or supervisors

Professsor Dr. Vesa Olkkonen, Minerva Foundation Institute for Medical Research

Säilytyspaikka – Förvaringställe – Where deposited

Ethesis service, University of Helsinki

Muita tietoja – Övriga uppgifter – Additional information

TABLE OF CONTENTS

ABBREVIATIONS

BiFC	bimolecular fluorescence complementation
ER	endoplasmic reticulum
FFAT	diphenylalanine in an acidic tract
HEK	human embryonic kidney
IP	Immunoprecipitation
IPTG	isopropyl -D-1-thiogalactopyranoside
LE/LY	Late endosomes/Lysosomes
LTP	Lipid transfer protein
MCS	Membrane contact sites
MSP	Major sperm protein
OCRL1	Oculo-cerebro-renal syndrome of Lowe 1
ORD	OSBP related domain
ORP	Oxysterol binding protein related protein
OSBPL	OSBP-like
OSPB	Oxysterol binding proteins
PBS	phosphate buffered saline
PH	pleckstrin homology
PI	phosphatidylinositol
PI4,5P	phosphatidylinositol 4,5-bisphosphate
PI4P	Phosphatidylinositol-4-phosphate
PIS	phosphatidylinositol synthase
PLC3	phospholipase C3
pmVC-C	C-terminal Venus fragment
pmVC-N	C-terminal Venus fragment (aa 155-238) fused at the C-terminus of the binding partners
pmVN-C	N-terminal fragment of Venus fluorescent protein
PPI	Protein-protein interactions
SDS-PAGE	sodium dodecyl sulfate polyacrylamide gel electrophoresis
T-ALL	T cell acute lymphoblastic leukemia cells

LIST OF TABLES

LIST OF FIGURES

1.Introduction

1.1 Oxysterol binding proteins

(OSPB) are a family of lipid binding/transfer proteins (LTPs). Most LTPs are ubiquitously expressed in human tissues but some show preference for one cell type over another. At least 10 families of LTPs have been recognized in the human genome. LTPs contain a lipid monomer accommodated by a soluble globular lipid transfer/binding domain the structural fold of which is specific to each family (Chiapparino, Maeda & Turei et al., 2016). As shown in Figure 1, the lipid binding domains which contain a hydrophobic lipid pocket may contain predominantly alpha helices or beta strands or similar amounts of both. For example, Im et al. (2005) showed that the yeast Osh4 proteins' lipid binding domain consists of both alpha helices and beta sheets, forming a hydrophobic tunnel that 'traps' the lipids inside. The lipid binding domains are typically covered by a 'lid' which can be in an open or a closed conformation. The lid opens when in contact with the membrane to facilitate the extraction of lipid molecules. Once the lipid is enclosed in the tunnel, the lid closes, and the protein is ready to transport the lipid to another membrane (Im, Raychaudhuri & Prinz et al., 2005; Lev, 2010).

OSBP was first discovered in mouse fibroblast cells as a cytosolic protein (Taylor, Saucier & Shown et al., 1984; Tong, Manik &Yang et al., 2016). Later, the cloning of rabbit OSBP (Dawson, Ridgway & Slaughter et al., 1989) helped identify a large family of OSBP-related proteins (ORPs; Laitinen et al. 1999; Lehto et al. 2001; Jaworski et al. 2001). At present, ORPs have been discovered in yeast, plants, mammals including humans and many other eukaryotes (Raychaudhuri & Prinz, 2010; Umate, 2011).

LTPs typically carry additional membrane binding determinants, such as a plecktrin homology (PH) domain, an ER-targeting motif, or a transmembrane segment. However, in ORPs such as the yeast ORP, Osh4, the lipid binding domain has two membrane interacting surfaces, one at the distal part of the sterol binding domain and another at the mouth of the sterol-binding pocket; this means it can bind two closely apposed membranes at the same time (Schulz, Choi & Raychaudhuri et al., 2009). In the case of Osh4, the pocket can bind either sterol or PI(4)P—two ligands that are exchanged between membranes by Osh4 (De Saint Jean et al. 2011 J Cell Biol).

Sterols are a type of lipid— others being glycerolipids, glycerophospholipds, fatty acids, sphingolipids, prenol lipids, and saccharolipids (Chiapparino, Maeda & Turei et al., 2016). Sterol lipids are further divided into cholesterol and its derivatives, steroids, secosteroids, bile acids and derivatives, and sterol conjugates (Fahy, Subramaniam &Murphy et al., 2008). Oxysterols are oxygenated 27-carbon derivatives of cholesterol that are synthesized during cholesterol metabolism (Bjorkhem & Diczfalusy, 2002). Although oxysterols present in biological membranes and lipoproteins are found in trace amounts —always in conjunction with excess cholesterol (10^3-10^6-fold), their presence can exert profound biological effects even at these low concentrations (Schroepfer, 1998; Bjorkhem & Diczfalusy, 2002; Christie, 2014).

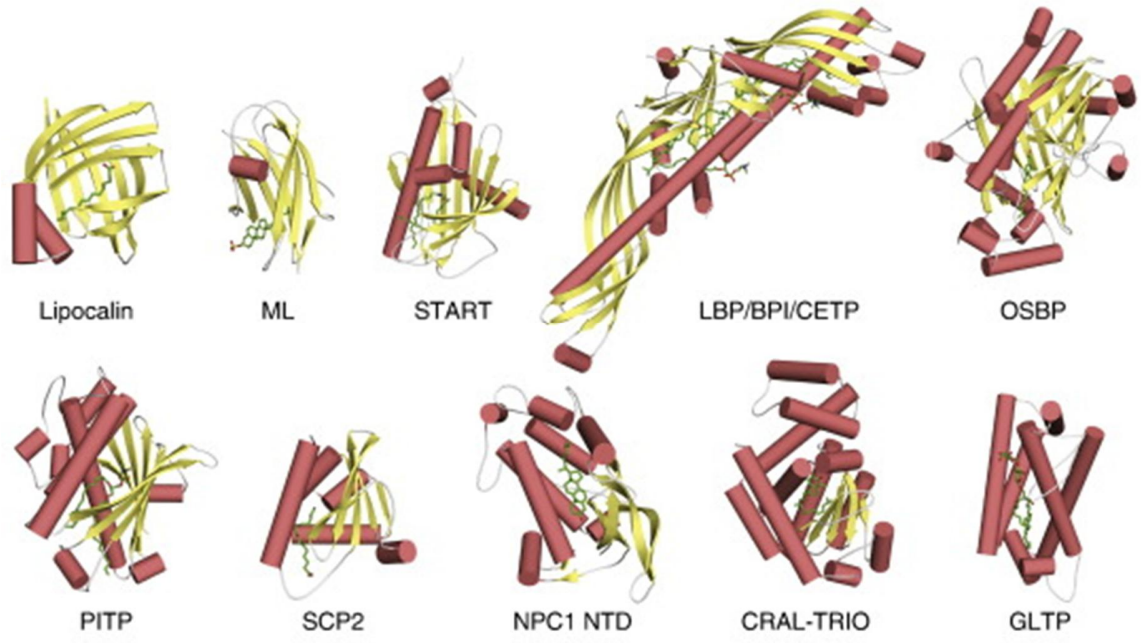

Figure 1. Cartoon displays of the three-dimensional structures of ligand-bound LTDs. The LTDs displayed are: the lipocalin domain of the rat FABP2 in complex with palmitate (PDB entry code 2IFB); the ML domain of the bovine NPC2 in complex with cholesterol sulfate (PDB entry code 2HKA, chain B); the START domain of the CERT in complex with C16-ceramide (PDB entry code 2E3O); the LBP/BPI/CETP domain of the CETP in complex with two molecules each of cholesteryl ester and phosphatidylcholine (PDB entry code 2OBD); the OSBP domain of the yeast Osh4 in complex with ergosterol (PDB entry code 1ZHZ); the PITP domain of the rat PITP in complex with PC (PDB entry code 1 T27); the SCP2 domain of the yellow fever mosquito SCP2-like 3 in complex with palmitate (PDB entry code 3BKR); the NPC1 NTD of the NPC1 in complex with cholesterol (PDB entry code 3GKI); the CRAL-TRIO domain of the TTPA in complex with α-tocopherol (PDB entry code 1R5L); and the GLTP domain of the GLTP in complex with lactosylceramide (PDB entry code 1SX6). The helices and β-strands are colored salmon and yellow, respectively. The bound ligands are shown as sticks with the carbon, nitrogen, oxygen, and phosphate atoms colored green, blue, red, and orange, respectively (Figs. 2–4) (figure obtained from Chiapparino, Maeda &Turei et al., 2016).

In humans, there are 12 genes encoding ORP proteins; whereas in yeast, only 7 genes encode ORPs. ORP proteins have several domains among which a C-terminal OSBP-related domain (ORD) is common to all. EQVSHHPP is the signature motif at the N-terminal part of the ORD. Apart from ORD at the C-terminal region, some ORPs also contain a diphenylalanine in an acidic tract (FFAT) motif, an alpha-helical region, a pleckstrin homology (PH) domain, ankyrin repeats, or a GOLD (Golgi dynamics) domain in the N-terminal region. In addition, the C-terminal region of mammalian ORP5 and ORP8 comprises a transmembrane segment (Lehto, Chinetti & Johansson et al., 2001; Beh, McMaster & Kozminski et al., 2012).

The ORD domain of several ORPs binds both sterol and phospholipids (Im, Raychaudhuri & Prinz et al., 2005). The first structure of an ORD domain was deciphered for yeast Osh4 protein with five different binding partners; cholesterol, ergosterol, 7-, 20-, and 25-hydroxycholesterol. Osh4 is a short 435 amino acid long protein lacking signature N-terminal domains such as a PH domain or FFAT motif. Residues 1-29 form the lid of the ORD, whereas the region immediately after it (30-117) is comprised of a two-stranded beta sheet and three alpha helices which surround the central beta barrel structure made by residues 115-293 (Raychaudhuri, Im & Hurley et al., 2006).

Members of the Oxysterol-binding protein family designated ORPs or OSBP-like (OSBPL) proteins are characterized by a C-terminal ORD. ORPs can be divided into long (L) and short (S) homologs based on the presence or absence of a PH domain respectively (Fig. 2) (Olkkonen & Li, 2013). The pleckstrin homology domain is around 120 amino acids long and present in the N-terminal part of the protein. These domains target ORPs to non-ER membrane compartments. The structures of all PH domains are somewhat similar even though the sequence similarity might be low. These domains contain an amphipathic helix and two beta sheets (Ferguson, Kavran & Sankaran et al., 2000). Most PH domains bind to phosphoinositides with affinities ranging from micromolar to nanomolar, and with different specificities (Ferguson, Kavran & Sankaran et al., 2000; Tong, Yang &Yang et al., 2013); in some cases, PH domains can also mediate protein-protein interactions.

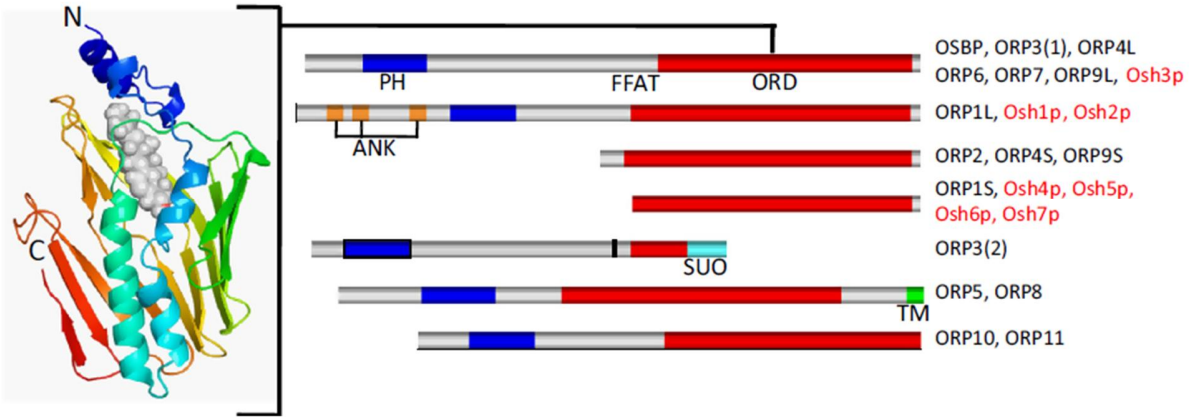

Figure 2. The major structural classes of mammalian and yeast *S. cerevisiae* ORP proteins. A molecular model of the ORP1 ligand-binding domain (ORD) generated by using the *S. cerevisiae* Osh4p structure [23] as template is displayed on the left. A beta-barrel-like fold forms a pocket closed by an alpha-helical lid, in which cholesterol (displayed in gray) is accommodated. ORPs belonging to each structural class are indicated on the right, mammalian proteins in black and yeast proteins in red print. PH, pleckstrin homology domain (membrane phosphoinositide binding); FFAT, two phenylalanines in an acidic tract motif (interaction with VAP proteins at the ER); ORD, OSBP-related ligand-binding domain; ANK, ankyrin repeats (putative protein interactions); SUO, sequence unrelated to ORD; TM, trans-membrane segment (anchoring to ER). Note: The structural classes do not correspond to mammalian ORP subfamilies I–VI dictated by relatedness in sequence and gene structure. (Olkkonen & Li, 2013).

1.2 FFAT Motif

FFAT is a conserved motif appearing in nearly all long ORPs. It contains the 7-amino acid consensus sequence EFFDAxE. Intracellular lipid traffic is mediated both by membrane vesicles and by a number of non-vesicular pathways facilitated by cytoplasmic lipid binding proteins (Loewen, Roy & Levine, 2003). However, for these binding proteins to function effectively, they must be targeted to specific membranes. FFAT acts as a targeting signal localizing a number of ORPs to the cytosolic face of the endoplasmic reticulum (ER) and to the nuclear membrane via the type II integral membrane protein VAP and its homolog, Scs2p, in yeast (Loewen, Roy & Levine, 2003; Kaiser, Brickner & Reilein et al., 2005). VAP is embedded in the ER through its C-terminal transmembrane domain, whereas the N-terminal Major sperm protein (MSP) homology domain binds to the FFAT sequence with assistance from a central coiled coil region (Kaiser, Brickner & Reilein et al., 2005).

1.3 Ankyrin Domain

Ankyrin repeats are 33 amino acid alpha helical motifs with a beta loop. The structure of this motif is conserved in most proteins although its function may vary. The beta loop of this motif plays a role in protein-protein interactions; because the ankyrin motif is involved in a number of different cellular functions, defects in these proteins have been found in a number of disease conditions (Mosavi, Cammett & Desrosiers et al., 2004). Among the mammalian ORPs, ankyrin repeats are only found in the N-terminal domain of ORP1L, while in yeast they are found in two long ORPs, Osh1p and Osh2p.

1.4 ORPs at membrane contact sites

Membrane contact sites (MCSs) are sites for exchange of lipids and signals between various intracellular organelles. Several ORPs localize and facilitate lipid transport over MCSs, and are also believed to act as lipid sensors at these sites. In ER-Golgi membrane contact sites, OSBP tethers the Golgi to the ER using its PH domain and FFAT motif, respectively. The ORD swings back and forth between the membranes to exchange PI(4)P for sterol. It uses the energy provided by the hydrolysis of PI(4)P in the ER to drive the transport of sterol from ER to the Golgi. Sac1 phosphatase in the ER membrane acts *in cis* to remove the phosphate group from PI(4)P, so that the PI(4)P gradient remains—thus maintaining the rate of cholesterol transport (Mesmin, Bigay & Moser et al., 2013). However, Sac1 phosphatase can also act *in trans* to regulate the concentration of PI(4)P in the plasma membrane. In yeast, Osh3p senses the plasma membrane PI(4)P level— then binds to Scs2p which in turn activates Sac1p activity *in trans* (Stefan, Manford & Baird et al., 2011). Similarly, ORP5 and ORP8 are integral membrane proteins of the ER that can bind to PI(4)P in the plasma membrane and transfer PS from the ER to the plasma membrane while transferring PI(4)P back to the ER, making the plasma membrane PS rich (Chung, Torta, & Masai, 2015).

ORP1L acts as a sensor of cholesterol. The availability of cholesterol in the outer membrane of Late endosomes/Lysosomes (LE/LY) determines the function of ORP1L in autophagosome-LE/LY fusion. ORP1L is recruited by Rab7 to the LE/LY (Johansson et bal. 2005 Mol Cell Biol). If the cholesterol level is low, the ORD domain of ORP1L is free from the membrane hence exposing the FFAT motif which is recruited by the ER protein VAP-A. This in turn blocks the fusion of autophagosome with LE/LY. If there is a high level of cholesterol, ORP1L binds it via its ORD domain and facilitates the recruitment of other tethering components to facilitate the LE/LY –autophagosome fusion. After the fusion of autophagosome and LE/LY to generate the new Amphisome/Autolysome, the Rab7 effector RILP recruits Dynein/dynactin for minus end-directed transport of these compartments. Again, low cholesterol levels can prevent the transport by releasing the ORP1L ORD domain and hence induce the binding of ORP1L to VAP-A in the ER (Wijdeven, Janssen & Nahidiazar et al., 2015; Rocha, Kuijl & van der Kant et al., 2009).

1.5 Oxysterol binding protein related protein 4 (ORP4)

ORP4 is a close homolog of OSBP. In humans, this gene is located on chromosome 22. It has three recognized variants, ORP4L, ORP4M and ORP4S. All together 23 exons are required to encode the full-length ORP4L protein. Alternate splicing from Exon 3 gives rise to the ORP4S variant which lacks a PH domain and a FFAT motif, and ORP4M which lacks the PH domain. ORP4 has high affinity for sterols: 7-ketocholesterol and 25-hydroxycholesterol. The binding of sterols to ORP4 is mediated by the OSBP related domain (ORD). ORP4 also interacts with vimentin intermediate filaments via the ORD and influences the localization and organization of vimentin (Ngo, Colbourne & Ridgway, 2010; Wyles, J., Perry, R., & Ridgway, N. (2007). Apart from sterol binding, ORP4 also binds PI(4)P *in vitro*. The silencing of ORP4 leads to reduced growth and survival of cells. This property of ORP4 promoting cell growth and survival is unique to this ORP (Charman, Colbourne & Pietrangelo, 2014).

ORP4 has been associated with a number of diseases. Hepatitis C virus is an RNA virus that infects hepatocytes and uses cellular lipids to replicate and cause pathogenesis of the host. ORP4 disturbs the viral replication by inhibiting an adaptor protein associated with the replication complex of the virus. In the presence of HCV, ORP4 also disturbs the lipid composition of the cell by increasing the number of lipid droplets, thus reducing the amount of lipids available in the ER for viral replication (Park, Ndjomou & Wen, 2013). Moreover, ORP4 was in early studies found up-regulated in circulating metastatic cancer cells and chronic myeloid leukemia cells (Fournier et al., 1999; Henriques Silva et al., 2003).

ORP4 was recently found to be crucial in oxidative phosphorylation and calcium homeostasis and hence the survival and proliferation of cervical carcinoma cell lines as well as of T cell acute lymphoblastic leukemia cells (T-ALL)(Charman et al. 2014; Zhong, Yi & Xu et al., 2016;). In T-ALL cells ORP4 is necessary to activate a target of G-protein coupled receptor, phospholipase C3 (PLC3), which regulates cellular calcium signaling and mitochondrial respiration. In other words, abundance of ORP4 fuels the energy for the cancerous T-ALL cells. Hence ORP4 can be viewed as a new target molecule for restricting the growth of theses cancerous cells (Zhong, Yi & Xu et al., 2016). In fact, other research has shown ORP4 as a target for molecules with anti-proliferative activities in tumor cells. These molecules, collectively known as ORPhilins, bind to OSBP and ORP4, which apparently has an anti-proliferative effect on cancer cells. ORPhilins compete for ORP4 binding of 25-OHC, suggesting that they bind within the sterol-binding pocket; Consistently, the addition of 25-OHC inhibits the activity of ORPhilins (Li, Xiao & Lai et al., 2016).

1.6 Phosphatidylinositol phosphates

Phosphatidylinositol, as its name indicates, is a lipid with an inositol ring. The inositol ring of this lipid is phosphorylated by various kinases to form Phosphatidylinositol phosphates (PIPs). There are in total seven types of PIPs generated by the addition of phosphate molecule on the 3, 4 or 5 positions of the inositol ring. The PIPs are essential signal transduction molecules. Some PIPs such as PI(3)P, PI(5)P, PI(3, 4)P2 and PI(3,5)P2 are far less abundant in cells compared to the others. PI(3)P is a hallmark of early and multivesicular endosomes where it carries out various functions in intracellular trafficking (Gillooly, Simonsen & Stenmark, 2001). Similarly, PI(3,5)P2 also plays an important role in endosomal dynamics by regulating actin on these organelles (Hong, Qi & Weaver, 2015). PI(5)P is esoteric as its localization is poorly understood, but it is by

far most common in the plasma membrane with the Golgi, ER and nucleus also being sites of its enrichment under certain circumstances (34). The others PIPs, mainly PI(4,5)P2 and PI(3,4,5,)P3 are localized in the plasma membrane where they act as substrates for a wide range of signaling proteins (Di Paolo & De Camilli , 2006). One of the best known PIPs is PI(4)P, which is localized in the Golgi complex and the plasma membrane and is a versatile regulator of lipid and vesicle transport. Its role in signaling, membrane trafficking, lipid metabolism and lipid transport has been quite thoroughly elucidated (Venditti, Masone & Wilson, 2016).

1.7 Phosphatidylinositol metabolizing enzymes

Phosphatidylinositol (PI) is the precursor for all phosphoinositides. PIs are synthesized in the ER membrane and ER membrane derived compartments by phosphatidylinositol synthase (PIS). PIS synthesizes PI by combining two of its substrates; CDP-DG and inositol (Kim, Guzman-Hernandez & Balla, 2011). As of now there are about 50 phosphoinositide metabolizing enzymes. PI kinases together with PIP phosphatases maintain the balance of cellular PIPs. These enzymes are prevalent in many tissues and multiple isoforms can work on several of the targets. However, the actual participation of enzymes in compensation is limited due to their different distributions in the subcellular compartments. (Staiano, De Leo &Persico, 2015).

1.8OCRL1

OCRL1 (Oculo-cerebro-renal syndrome of Lowe 1) is a 901 amino acid protein located in X chromosome in humans. This protein consists of 4 major domains; N-terminal Pleckstrin homology (PH) domain, centrally located inositol polyphosphate 5-phosphatase and ASH domains, and a C-terminal domain homologous to Rho protein. This protein is one of the 10 phosphatases responsible for dephosphorylating the 5’ phosphate from the inositol ring of PIPs. The domain organizations of these phosphatases are shown in Figure 3. OCRL1 and Inpp5b have a similar domain organization and are closely related to each other. Although substrates for both of these proteins are similar and they are more inclined to dephosphorylate PI(4,5)P2, OCRL1 can sense the fatty acids of the lipid substrate whereas Inpp5b cannot. In addition, OCRL1 and Inpp5b both act on PI(3,4,5)P3 but only OCRL1 shows activity towards PI(3,5)P2 (Schmid, Wise & Mitchell, 2004). Although the substrates of OCRL1 are limited to the plasma membrane and the endocytic pathway, OCRL1 localizes to the Golgi complex as well. It also resides on endosomes and endocytic vesicles by binding to the endocytic proteins APPL1 and Ses1/2. OCRL1 also interacts with clathrin (Pirruccello, & De Camilli, 2012).

OCRL1 is associated with a rare X-linked disease called the Lowe syndrome. The occurrence of Lowe disease is approximately in 1 every 500,000. The Lowe syndrome is a multisystem disorder characterized by a congenital eye defect, mental retardation causing behavioral problems and defective proximal tubules of the kidney (Lowe, 2005). Type 2 Dent disease which is characterized by dysfunctional renal proximal tubule is another disease caused by mutations in OCRL1. Reduction of PIP phosphatase activity and accumulation of the OCRL1 substrate PI(4,5)P2 are common in the fibroblasts of these patients (Lowe, 2005).

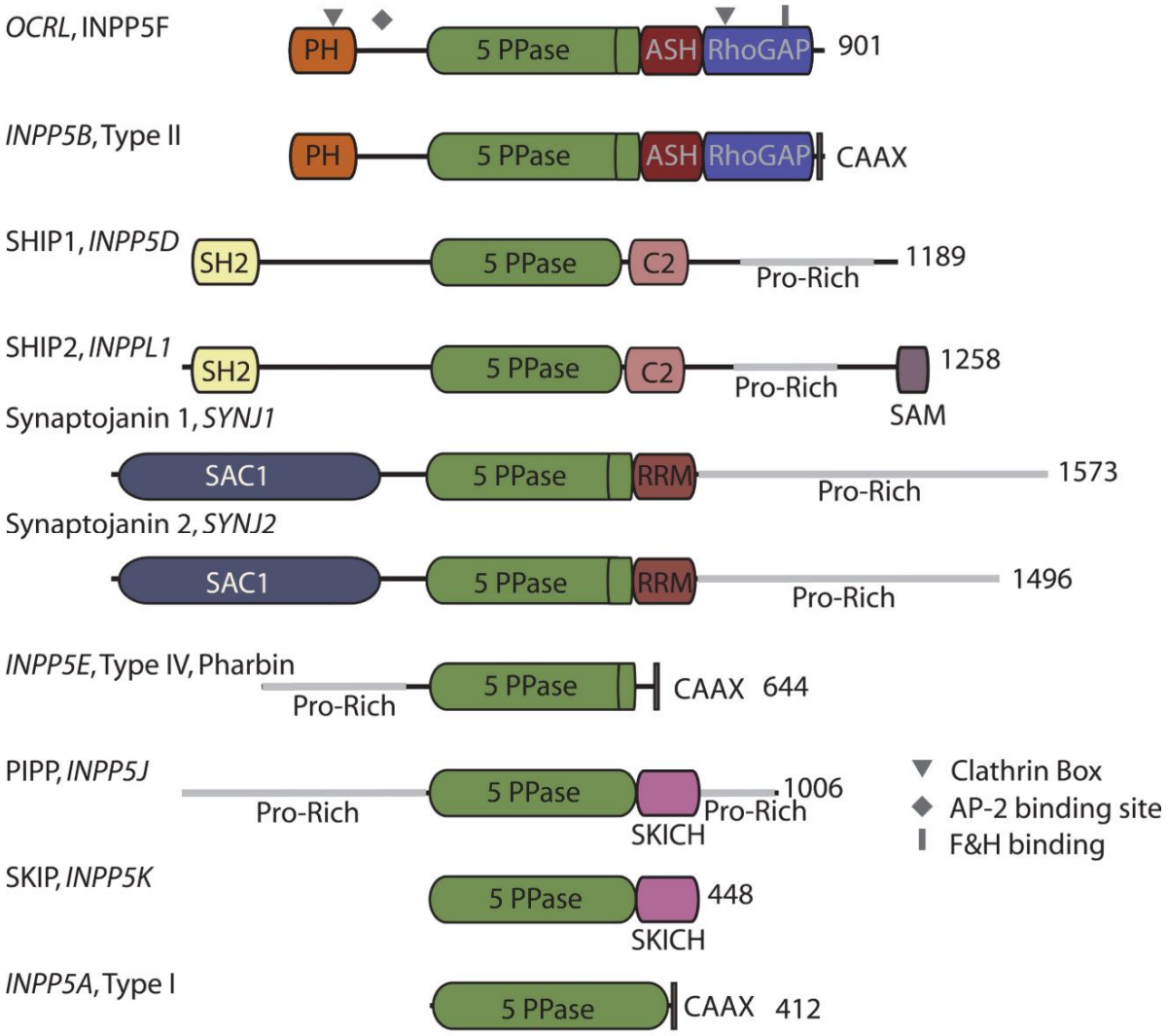

Figure. 3. The domain structures of PIP 5'-phosphatases. From: Pirruccello et al., Nat Struct Mol Biol REF

2. Aims of the Study

This study generally aims to demonstrate the interaction of ORP4 with OCRL1 through *in vitro* biochemical studies. In particular, this study aims to transfect HEK 293 cells with plasmid DNA containing the gene that codes for the ORP4 and OCRL1 proteins. Protein interactions will be demonstrated through co-immunoprecipitation and western blot. Finally, bimolecular fluorescence complementation (BiFC) shall be employed to directly visualize the resulting protein interactions.

3. Materials and Methods

3.1 Cell Line and Cell Culture

3.1.1 Culture of HEK293 cells

The experiments were performed in human embryonic kidney (HEK) 293 cells (American Type Culture Collection, ATCC, CRL-1573). The cells were cultured in Dulbecco's Modified Eagle's medium –low glucose (DMEM, Sigma-Aldrich®, St. Louis, MO, USA), 10% fetal bovine serum (FBS; Gibco/Invitrogen, Grand Island, NY, USA), 100 U/ml penicillin and 100 ug/ml streptomycin, 8 m200 mM L-Glutamine. The cells were maintained at constant temperature of 37°C with 5% CO2 and humidity in an incubator.

3.1.2 Freezing and recovery of cells

Cells were centrifuged at 1,200 rpm for 3 minutes, the pellet was collected in 10% FBS-DMSO (9:1) and frozen in 1 ml aliquots inside Cryo.s™ Cryogenic storage vials (Greiner Bio-One, Frickenhausen, Germany) first at -80 °C for one day and then at -140 °C permanently.Cells were rapidly thawed at 37 °C in a water bath. 10 ml of phosphate buffered saline (PBS) was added to 1 ml of cells and mixed gently using pipette. The cells were centrifuged at 1200 rpm for 3 minutes. The supernatant was discarded and the pellet was resuspended in 10 ml of DMEM with the above supplements and maintained in T75 flasks (Cellstar® Greiner Bio-One, Frickenhausen, Germany).

3.1.3 Transfection of cells

For HEK293 cells, transfection using Lipofectamine 2000™ (Invitrogen, Carslbad, CA, USA) was employed. Transfection was performed either in 6-well plates for pull down and co-immunoprecipitation (IP) experiments or in 24-well plates for imaging. First, cells were cultured until 70-80% confluency. For 6-well plates, 10 ul of Lipofectamine 2000 was diluted in 250 ul of Opti-MEM (Thermo-Fisher Scientific, Waltham, MA, USA) and kept at room temperature for 5 minutes. A maximum of 4 ug of DNA was diluted in 250 ul of Opti-MEM. Diluted DNA was then added to diluted lipofectamine in 1:1 ratio and incubated for 30 minutes at room temperature. The DNA-lipid reagent complex was added to HEK293 cells and incubated at 37 °C for 20-24 hrs. Similarly, for 24-well plates 2 ul of Lipofectamine 2000 was diluted in 50 ul of Opti-MEM and kept at room temperature for 5 minutes; A maximum of 0.8 ug of DNA was diluted in 50 ul of Opti-MEM. Diluted DNA was then added to diluted lipofectamine in 1:1 ratio and incubated for 30 minutes at room temperature. The DNA-lipid complex was added to HEK293 cells and incubated at 37 °C for 20-24 hrs.

3.2 Cell Lysis

Cell were washed with ice cold PBS and lysed with 1ml of lysis buffer (10 mM HEPES pH7.6, 150 mM NaCl, 0.5 mM MgCl2, 10% glycerol, 0.5% Triton X-100, 1mM DTT, Protease inhibitor cocktail (Roche Diagnostics, Basel, Switzerland).

3.3 Pull down assay

Pull down assay was used to confirm binding and interacting partners of ORP4 protein. Constructs with HA (Thermo-Fisher Scientific) or FLAG (Sigma-Aldrich, Saint Louis, MO, USA) tags were used as baits to confirm the binding partners as well as to study the protein interaction. 1 ml of cell lysates were collected in 1.5 ml Eppendorf tubes, which were rotated in a rotator for 15 minutes in a cold room. The lysates were then centrifuged at 13,000 rpm for 5 minutes at 4 °C to separate a soluble total cell protein/protein complex fraction from the debris pellet. 50 ul of total input protein was collected from each sample in a separate tube and 10 ul of 6X Laemmli sample buffer (LSB): (10 ml LSB: 1.2 g SDS, 6 mg bromophenolblue, 4.7 ml glycerol, 1.2 ml 0.5M Tris pH6.8, ddH20, 0.93 mg DTT) was added. Magnetic beads were washed 3 times with 1 ml of lysis buffer, and 20 ul of antibody tagged magnetic beads were added in each tube containing lysate to precipitate the protein with specific tags. The tubes were subjected to gentle rotation for 1 hour in a cold room. Magnetic beads containing associated protein complexes were washed 3 times with 1 ml lysis buffer using a Dynal® magnetic rack (Invitrogen, Thermo- Fisher). The proteins bound to magnetic beads were eluted with 40 ul of 1X reducing LSB; first the beads were boiled for 5 minutes and then centrifuged 5 minutes at 13,000 rpm. The magnetic beads and LSB containing the proteins of interest were separated using a magnetic rack.

3.4 Immunoprecipitation

Co-immunoprecipitation is a powerful tool to confirm interacting partners of a protein. Here, it was used to confirm the association between ORP4 and OCRL1.These proteins were fused with specific epitopes like FLAG (DYKDDDDK), HA (haemagglutinin, YPYDVPDYA) or a fully functional protein like the 27kD green fluorescent protein (GFP) protein. The fusion proteins were overexpressed in HEK293 cells. The total cell lysates were collected as described above. 50 ul of lysate was collected in a new tube for total protein expression observation. 2 ug of antibody was added in the rest of the lysate and subjected to overnight gentle mixing at 4 °C. Here the antibody binds to specific antigens present in the fusion protein. The next day, 20 ul of anti-HA or anti-FLAG magnetic beads was added to the same tube and mixed gently on a roller for 2 hrs. The magnetic beads were then washed 2X with lysis buffer and once with similar buffer without DTT and Triton X-100. 40 ul of 1X LSB was added to the beads containing possible protein complex. The sample was then boiled for 5 minutes and centrifuged for 5 minutes at full speed in a microcentrifuge. The protein complex is contained in the LSB. The magnetic beads are thereafter discarded and the LSB containing the proteins is further analyzed by western blotting.

3.5 Western Blotting

The proteins collected from immunoprecipitation or pull-down assay were further analyzed by western blotting. At first SDS-PAGE was run to separate proteins by their molecular weight. 1.5 mm gel with 12% resolving gel* (3ml 40% acrylamide (29:1) 4.5ml MilliQ water, 2.5ml of 1.5M Tris pH 8.8, 10% SDS 100 ul, 10% APS 100 ul, 4 ul TEMED per gel) and 5% stacking gel* (500 ul 40% acrylamide:bis-acrylamide (29:1), 3 ml milliQ water, 512 ul 1M Tris pH 6.8, 42 ul 10% SDS, 42 ul 10% APS, 4 ul TEMED per gel) was cast using Mini-PROTEAN 3 Multi-Casting Chamber (Bio-Rad). Electrophoresis apparatus was assembled with gel and

electrophoresis buffer* (125 mM Tris Base pH 8.3, 1.25M glycine, 0.5% SDS). 30 ul of total input protein and 20 ul of pull down or IP sample (unless otherwise stated) were run in the gel first at voltage 60V for the sample proteins to concentrate together in the stacking gel and then at 120V for the resolving gel. The samples were transferred to Nitrocellulose membrane which was submerged in transfer buffer before the transfer. A sandwich-like complex was assembled with filter paper on both sides of the gel and membrane. The sandwich was placed in a chamber filled with blotting buffer. The transfer was performed either for 90 minutes at 400 mA at 4 ℃ or overnight in 40 A at 4°C. The membrane was blocked with 50 ml of 5% milk in TBS--T (Tris-buffered saline with 0.1% Tween-20) * and shaken on a with a see-saw rocker. 5 ml of primary antibodies were prepared in TBS-T and incubated with membrane at room temperature for an hour. The membrane was washed with TBS-T for 5 minutes and repeated two more times. 5 ml of secondary antibody conjugated with Horseradish peroxidase were prepared in TBS-T and incubated with the membrane for 45 minutes – 1 hour. The membrane was washed for 5 minutes and repeated two more times. Enhanced chemiluminescence substrate (Pierce, Thermo Scientific) was used to visualize the blot. After two minutes the blots were taken to the dark room to be visualized with Carestream (Kodak, Sigma-Aldrich) developer and replenisher.

3.6 Fluorescence microscopy

The cells were grown and transfected using the methods described in the transfection section. After 24 hours of transfection cells were washed with phosphate buffered saline (PBS) and fixed with 4% paraformaldehyde in PBS for 25-30 minutes. The cells were then washed with PBS, and 0.5 ml of 50 mM NH_4Cl was added for 10-15 minutes. The cells were washed with PBS, and 0.5 ml 1% TritonX-100 was added for 5 minutes to permeabilize the cells. The cells on coverslips were again washed with PBS and transferred to a humidified chamber with the help of forceps and a needle. 10% FBS in PBS was used to block unspecific binding of antibodies. The humidifier chamber was kept in room temperature for 45 minutes. Primary antibody was diluted in 5% FBS-PBS. 70-90 ul was added to the coverslips and incubated in 37ºC for 45 minutes. The coverslips were washed 3 times for 5 minutes each with PBS. Fluorescent secondary antibody conjugates (Alexa488, Alexa568; Thermo Scientific) were diluted in 5% FBS-PBS and added on the coverslip. After 45 minutes of incubation at room temperature the coverslip was washed for 5 minutes with PBS 3 times. Then the coverslips were mounted with MowiolTM (polyvinyl alcohol, Sigma-Aldrich) containing 1,4-diazobicyclo- [2.2.2]-octane (DABCO, Sigma-Aldrich) for improving the lifetime of dyes and DAPI for staining the nucleus. Zeiss Axio observer Z1 microscope was used for capturing the images using the above above-mentioned method with fluorescence dyes. Pln Apo 63X oil/1.4 oil DICII objective lens with colibri laser were used to observe the fluorescence. ZEN 2 (Blue edition) software was used to take the images. Pln Apo 63X oil/1.4 oil DICII objective lens with colibri laser were used to observe the fluorescence.

3.7 Bimolecular fluorescence complementation

Bimolecular fluorescence compensation (BiFC) is a technique for visualizing protein-protein interactions or proximity. pmVN-C; N-terminal fragment of Venus fluorescent protein (aa 1-172) fused at the N- terminus of ORPs were paired with pmVC-C; C-terminal Venus fragment (aa 155-238) fused at the N-terminus of the binding partners or pmVC-N; C-terminal Venus fragment (aa 155-

238) fused at the C-terminus of the binding partners. The vectors used for generating the Venus fragment fusion constructs are depicted in Figure 4. The fusion proteins were expressed in cells via double transfection as specified above.

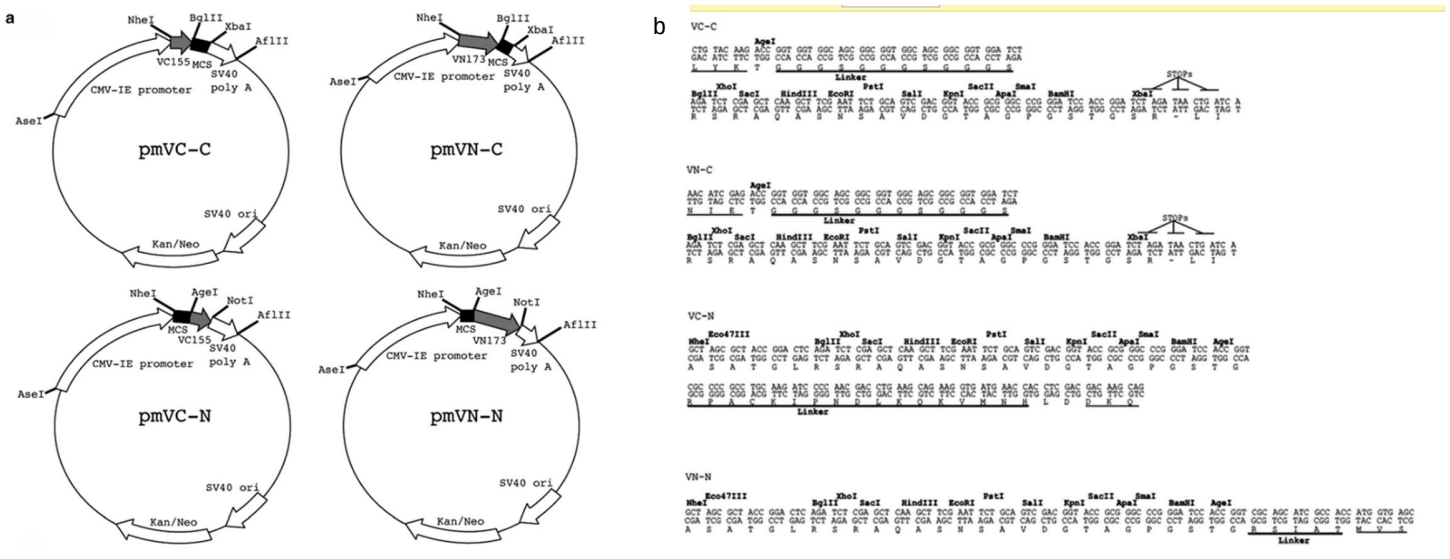

Figure 4. Mammalian plasmid maps and sequences of the multiple cloning sites. Mammalian plasmids enable high-level transient expression of the target protein tagged either at the amino (VC-C and VN-C)- or carboxy (VC-N and VN-N)-terminus with Venus fragments. Underlined single-letter amino acid sequence is Venus sequence. Unique restriction enzyme sites are shown in *bold* (Weber et al., 2015; Yeast *Saccharomyces cerevisiae* and mammalian cells)

3.8 Subcloning of full-length the OCRL1 and OCRL1 ASH domain constructs (see Table 3, List of plasmids)

Molecular cloning with SalI/BamHI restriction enzymes was performed to transfer the OCRL1 cDNA from HA-OCRL1 vector into pmCherry vector (Fig. 5) and pmVC-C vector (Fig. 4) to tag the N-terminus of OCRL1with mCherry and C-terminal fragment of Venus fluorescent protein, respectively. Similarly, ASH domain PCR product of OCRL1 was cloned into the pGEX4T-1 vector to place the ASH domain as a fusion at the end of GST. To tag OCRL1 at the C-terminus with eGFP or with three Flag tags, the OCRL1 open reading without stop codon was PCR amplified with plasmid 1499 as template and cloned into pEGFPN1 with SalI/BamHI enzymes or pcDNA3.1-3xFLAG with BamHI/XhoI. Venus C-terminal fragment was added at the C-terminus of OCRL1 by transferring the cDNA without stop codon from plasmid 1508 to pmVC-N with SalI/BamHI.

3.8.1 Primer design and polymerase chain reaction

The primers for amplifying the full human OCRL1 open reading frame (NCBI accession number BC094726) or the ASH domain were designed for ASH domain of human OCRL1 (NCBI accession number BC094726). OCRL1 is 2682 nucleotides long and the ASH domain is encoded between nucleotides 1689 and 2034. The forward and reverse primers (Table 1) were designed according to suitable restriction sites to facilitate cloning

of start and stop codons, as well as BamHI and SalI sites for multiple cloning sites of pcDNA3.1-3xFLAG, pEGFPN1 or pGEX4T-1 vectors.

Table 1. The primers used for generating human OCRL1 and OCRL1 ASH domain constructs

Primers sequences	Length	Tm(^{0}C)	% GC content
Forward Primer for OCRL1			
5'TGCA**GTCGAC**ATGGAGCCGCCGCTCCCGGTC3'	31	72.3	71
Reverse Primer for OCRL1			
5'CGGT**GGATCC**GTCTTCTTCGCTCCCAAGCAG3'	31	68.3	61
Forward Primer for ASH			
5'TTTT*GGATCC*ATGTCCTTAGAACTCAGCAGGAGG3'	34	64.1	47
Reverse Primer ASH			
5'TTTT*GTCGAC*TAAACTTGGGAGGTAATTTCCACTG3'	35	62.1	40

Table 2. **Polymerase chain reaction program**. Polymerase chain reaction was performed using C1000 touch Thermal Cycler by Biorad, by using the following program:

1. 98^0 C for 5 min
2. 98^0 C for 1 min
3. 54^0 C for 45 sec
4. 68^0 C for 4 min
5. 72^0 C for 15 min
6. 4^0 C on hold

Step 2-4 was cycled 25 times

3.8.2 Ligation and Transformation

PCR cleanup was performed using protocol and equipment provided by Nucleospin gel and PCR cleanup kit (Macherey-Nagel, Düren, Germany) by Biotop. Vectors and inserts were cut using same Fast DigestTM enzyme (Thermo Scientific) to match each other. In this case for all the cloning reactions BamHI and SalI were used. 2 ul (1-3 ug) of plasmid DNA insert, 0.5 ul of BamHI and 0.5 ul of SalI, 2 ul buffer and 15 ul of H2O was used to perform restriction digestion at 370 oC. Ligation was performed overnight at 16 oC using 11.5 ul of insert DNA (3-5-fold molar excess as compared to vector), 1 ul of vector DNA (about 50 ng), 1.5 ul ligase buffer and 1 ul T4 DNA ligase enzyme (Ppromega, Madison, WI, USA).

The constructs were transformed in New England Biolabs (Ipswich, MA, USA) EB 5-alpha competent *E. coli* cells. 25 ul of NEB5-alpha was thawed on ice for 10 minutes. 1.5 ul of construct was added to the tube and

mixed carefully by flicking 4-5 times. It was kept on ice for 30 minutes. The competent cells with vector was then heat shocked for 1 minute at 420 C and kept on ice for 5 minutes. 250 ul of SOC media was added to the mixture and placed at 370 C for 1 hour in shaking at 250 rpm. For ASH construct, 50 ul of the the cells were added to Luria-Bertani (LB) Ampicillin (100 ug/ml) selection plates whereas for OCRL1 constructs, 50 ul of the cells were plated on LB Kanamycin (30 ug/ml) resistant LB medium since both mCherry and pmVC-C vectors carry a Kanamycin selection marker. The plates were kept in 37 °C overnight in an incubator. Individual colonies from each plate were picked in 5 different tubes and grown in 3 ml of LB medium with Ampicillin. It was then left for overnight incubation at 37 °C with shaking at of 250 rpm. Plasmid Miniprep DNA was prepared for all 5 of the colonies using Nucleospin® Plasmid isolation kit (Biotop). 2 ul of DNA sample, 0.5 ul of BamHI and 0.5 ul of SalI, 2 ul 10x buffer and 15 ul of H2O was used to perform restriction digestion of the sample at 37 °C. The samples were run in 1% Agarose in Tris-Acetic acid-EDTA (TAE) buffer. The sample with correct band size was chosen for all the constructs. GST tagged ASH domain in pGEX4T.1 vector was further purified for pull-down assays.

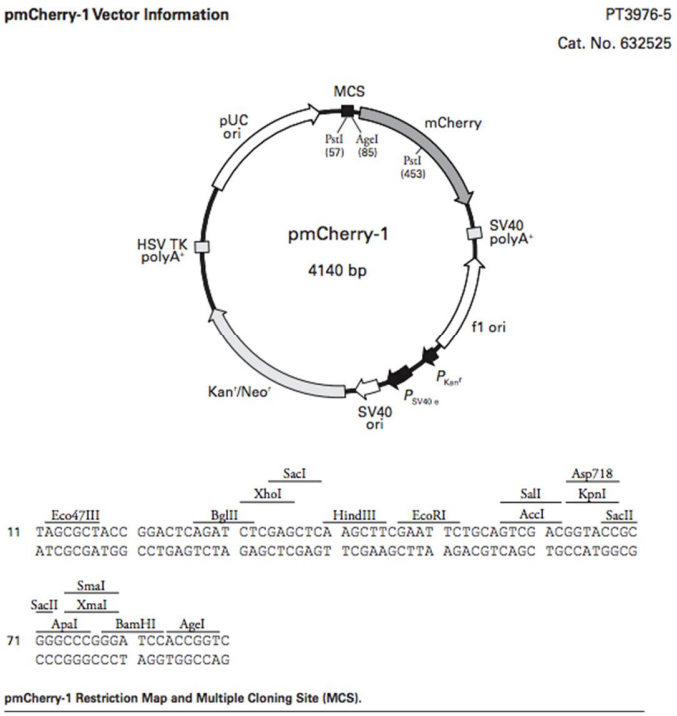

Figure 5. Map of pmCherry-1; Source: Clontech

3.9 Protein production and purification of the OCRL1 ASH domain

ASH domain in pGEX4T-1 vector (Fig. 6) was transformed into *E. coli* Rosetta competent cells according to the NEB5-alpha protocol described in section 3.7.3. The next day the plate was scraped with a scraper and the contents were added into conical flask with 500 ml of LB broth media containing Ampicillin. The cells were grown in 37 oC with constant shaking till the OD600 value was between 0.5-0.6. After the cells reached the

desired OD value expression of GST-ASH domain was induced with 1mM isopropyl -D-1-thiogalactopyranoside (IPTG) for 4 hours. The cells were centrifuged at 4500 rpm for 20 minutes. Then they were lysed with 25 ml of lysis buffer (20 mM HEPES, 250 mM NaCl, 0.5% Triton X-100, DNAse 1, 1 ug/ml, Lysozyme, 1mg/ml, Roche protease inhibitor cocktail, 1 tablet). The lysate was then centrifuged at 40,000 rpm for 20 minutes and supernatant was collected. GSHT beads were washed with lysis buffer. 1.3 ml of GSHT beads were added to 20 ml of cleared supernatant and rotated overnight at 4 0 C. Polyprep chromatography column (0.8 x 4 cm; BioRad, Hercules, CA, USA) was set up using a stand, and the GST beads containing ASH protein was poured into the column. Once the supernatant drained the column was washed with 10 ml wash buffer (20 mM HEPES, 250 mM NaCl, 0.5% TritonX-100) 4 times. The GST tagged ASH was eluted with 10 mM glutathione in Tris buffer. Ten fractions of 1 ml each were collected in different tubes. 20 ul of each fraction was taken in a new Eppendorf tube and 4 ul of 6X LSB was added to it, followed by boiling for 5 minutes and centrifugation for 5 minutes at 13000 rpm. SDS-PAGE gels were run and stained with Coomassie blue and the bands were checked.

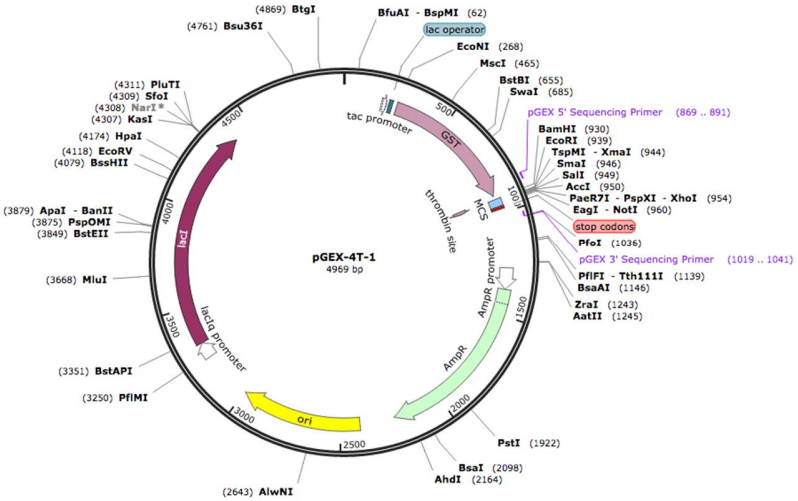

Figure 6. Map of the pGEX-4T-1 vector; Source: Snapgene

Table 3. List of Plasmids.

Plasmid	Name	Species	Insert	Tag	Source	Original Vector
1499	HA-OCRL1	Human	OCRL1	HA, N-terminal of OCRL1	Addgene #22207	pcDNA3.1
1493	VA-HAORP4	Human	ORP4L	VN, N-terminal of ORP4	M. Weber-Boyvat	pmVN-C
1497	VA-ORP4	Human	ORP4L	VN, N-terminal of ORP4	Weber-Boyvat et al. 2015	pmVN-C
1507	mCherry-OCRL1	Human	OCRL1	mCherry, N-terminal of OCRL1	This study	pmCherry-1

1508	VB-OCRL1	Human	OCRL1	VC, N-terminal of OCRL1	M. Weber-Boyvat	pmVC-C
1480	VA-HA ORP4 mPHD	Human	ORP4mPHD	VN + HA, N-terminal of ORP4mPHD	M. Weber-Boyvat	pmVN-C
1479	VA-HAORP4ΔELSR	Human	ORP4mPHD	VN + HA, N-terminal of ORP4ΔELSR	M. Weber-Boyvat	pmVN-C
1658	OCRL1pcdna3.1-3XFLAG	Human	OCRL1	3xFLAG, C-terminal of OCRL1	This study	pcDNA3.1
1659	OCRL1-VB	Human	OCRL1	VC, C-terminal of OCRL1	This study	pmVC-N
1657	OCRL1-eGFP	Human	OCRL1	eGFP, C-terminal of OCRL1	This study	eGFP
1339	VB-VAPA	Human	VAPA	VC, N-terminal of VAPA	Weber-Boyvat et al. 2015	pmVC-C

4. Results

4.1 SDS-PAGE Electrophoresis and western blot of GST-ASH with ORP4

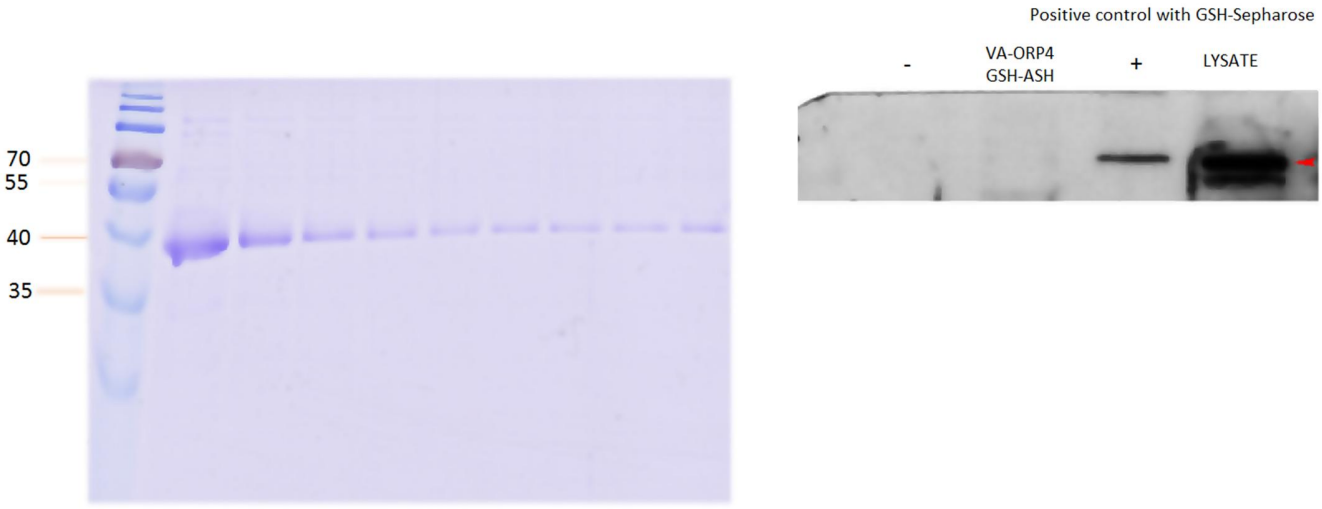

Figure 7. (a) **SDS-PAGE electrophoresis and staining of GST-ASH domain of OCRL1.** SDS-PAGE gel showing GST-ASH tagged protein in each elution fraction 1-9 of the Agarose column used for the purification. Molecular markers of known size in kDA are on the left. Results of the GST-ASH protein purification indicate the presence of the GST tagged ASH (GST 26kD + ASH domain 13.3 kD) as indicated by the band at ~ 39 kD in Coomassie stained gel. (b)

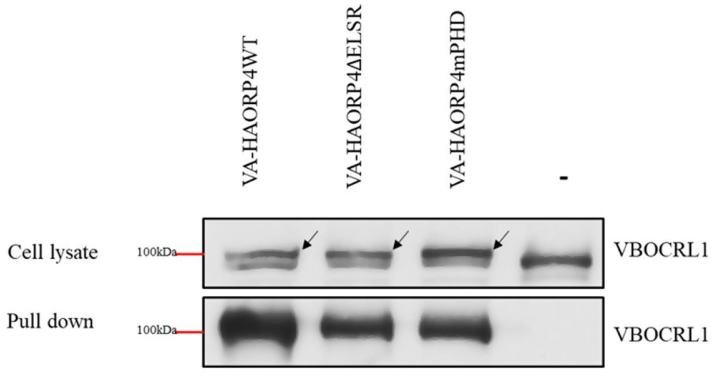

Figure 8. **Detection of protein expression and interaction by co-immunoprecipitations and Western blotting**. VA-HA-ORP4L and VB-ORCL1 were overexpressed in HEK293 cells, and immunoprecipitation was carried out with anti-HA. The negative control sample in the 4th lane contained no VA-HA-ORP4L. ORP4 and ORP4 mutant fusion proteins were identified with HA antibody, and OCRL1 with a specific OCRL1 antibody. The top bands indicated by arrow represent overexpressed ORP4L.

The top-most band in the cell lysate lanes of Figure 12 represents ORP4 not detectable in the negative control (-). The higher mobility band is an unknown cross-reactive protein. Below, the pull-downs done using HA magnetic beads, probed with OCRL1 antibody, are shown. The results confirm the interaction between OPR4 and OCRL1 suggested by the BiFC assay, and also show interaction between the sterol- and phosphoinositide-binding deficient mutants of ORP4 with OCRL1, suggesting that these functions are not crucial for the interaction of ORP4L with OCRL1.

4.2 BiFC analysis demonstrates interaction of ORP4L and OCRL1

ORP4L is one of the three variants of oxysterol-binding protein related protein 4 (ORP4), which is a lipid-binding transport protein G-protein coupled signaling and is essential in cell proliferation and survival. In the human genome, ORP4 is involved in the transport of lipids inside the cell in association with phosphatidylinositol-4-phosphate (PI4P) (De Craene et al., 2017). OCRL1, on the other hand, is an amino acid that is one of the 10 phosphatases involved in the dephosphorylation of phosphatidylinositol 4,5-bisphosphate (PI4,5P), thus yielding phosphatidylinositol-4-phosphate (PI4P) in the process. The association of ORP4 with PI4P, a product of the activity of OCRL1, therefore suggests a possible interaction between ORP4L and OCRL1.

This interaction could be directly visualized through BiFC analysis. Using fluorescent proteins fused at the N-terminus of ORP4L (VA-ORP4L) and C-terminus of OCRL1 (VB-OCRL1, OCRL1-VB), interaction between the two proteins could be observed. Figure 9 shows the co-expression of VA-ORP4 with OCRL1-VB (Fig. 9c) and co-expression of VA-ORP4 with VB-OCRL1 (Fig. 9c).

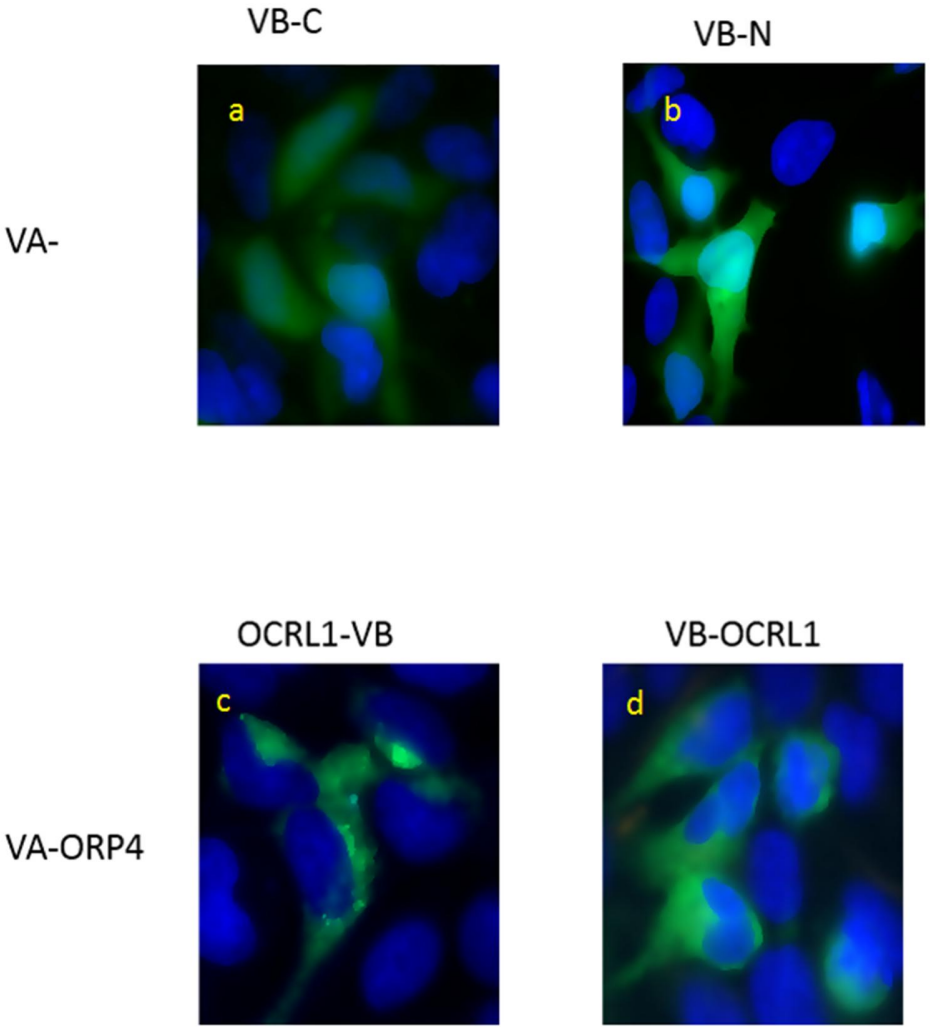

Figure 9. Interaction of ORP4L and OCRL1 as seen in BiFC analysis. a and b are tagged controls where VA tag is the N-terminal fragment of Venus fluorescent protein (aa 1-172) and the VB tag is the C-terminal Venus fragment (aa 155-238). c) Co-expression of VA-ORP4 with OCRL1-VB. d) Co-expression of VA-ORP4 with VB-OCRL1. The nuclei are stained with DAPI.

5 Discussion

The results of the BiFC analysis indicate that interaction between the ORCRL1 and ORP4 is dependent on the orientation of the protein pairs expressed in HEK293 cells. When fusion of both the ORP4 fragment and the OCRL1 fragment took place downstream from the Venus fluorescence tag (Figure 9 d), the resulting signal was weak and did not significantly differ from the negative controls (a, b). A more specific-appearing signal was obtained when the orientation was downstream of the fluorescence tag for ORP4 and upstream of the tag for OCRL1 (Figure 9).

SDS-PAGE detection of the GST-ASH domain of OCRL1 fusion protein

SDS-PAGE results confirm the production and purification of the GST-ASH domain tagged protein in all of the eluate fractions (Fig. 7). Coomassie stain clearly reveals the presence of the tagged ASH domain of OCRL1 by weight. The left lane provides molecular weight markers and the GST-ASH is confirmed present at ~39 kD. The ASH domain of OCRL1 has a molecular weight of 13.3 kD while the GST tag ~ 220 amino acids long, has a weight of 25 kD confirming the likely fusion of the tag to the ASH domain of OCRL1. The results do suggest that the ASH domain was tagged with GST.

Immunoprecipitation and Pull-down assays

Immunoprecipitation (IP) can be done using either pre-immobilized or free antibodies ("Overview of the Immunoprecipitation (IP) Technique | Thermo Fisher Scientific", 2018). Although both methods are chromatographic in nature and both are done using a bead matrix, in the case pre-immobilized IP monoclonal or polyclonal antibodies which target a specific protein, the antibodies are immobilized on a solid support (in this study anti-HA magnetic beads were used). The beads are then incubated under gentle agitation with a lysate solution containing the target protein. During this time the antigen target binds to the antibody which is immobilized on the column. Following the incubation period, the antibody-antigen complexes which formed are eluted from the column and analyzed. The free antibody method also involves use of an immobilized support; but only after the antibody and unbound antigen have been incubated and allowed to form immune complexes freely in lysate. The beads are then used to retrieve the complexes. However, it would be interesting to investigate whether the free antibody technique might have yielded different results.

Complexes may not be detectable in a co-immunoprecipitation or pull-down assay if the target proteins are present at very low concentration, if the antibody has a weak binding affinity to the antigen or if the kinetics for the antibody-antigen pair complex formation are too slow for the pull down ("Overview of the Immunoprecipitation (IP) Technique | Thermo Fisher Scientific", 2018). In the present co-IP experiments, we aimed to precipitate pre-formed cellular VA-HA-ORP4L-VB-OCRL1 complexes with anti-HA antibody. The presence of clear bands at 100kD indicate that it is likely that the complexes between OCRL1 and the OPR4 and OPR4 mutants were present. The band was absent in the negative control, evidencing for specificity.

The evidence from the co-IP assays indicates that VA-ORPL4 and its mutants DELSR (sterol binding abolished) and mPHD may all have interacted with ORCL1. Although the assay showed no separation of bands for either the OPR4 or the mutants with OCRL1, there was a separation of bands when the complexes were allowed to form freely in the lysate. Column separation could have been hindered by kinetics (if exchange was fast) or by solutions that were too dilute. However, the GST tagged ASH domain of the OCRL1 showed up on the SDS-PAGE and in general, Commasi blue has a lower detection threshold for proteins than Western Blot. Commasi blue detects complex formation at 8-10 ng for some proteins and 25 ng per band for most proteins ("Protein Gel Staining Methods | Thermo Fisher Scientific", 2018).

The results of the BiFC assay indicates the possible interaction of OCRL1 and the ORP4L protein overexpressed in the HEK293 cells, which was orientation dependent with respect to the fluorescence tag (Figure 9 c,d). Only the OCRL1 protein fused upstream of the fluorescent tag paired with the OPR4 fragment that was fused downstream of tag gave good signal in the BiFC assay indicating the possibility of PPI in this instance. However, it is also possible that the some or all of the fluorescence signal observed in Figure 9 may result from nonspecific interaction such as random collision of overexpressed, non-interacting protein fragments. The assay was not done quantitatively and only 2 of the 8 possible combinations of fusion proteins were examined; Kerppola, Jackson & Sanders (2009), Kodama and Hu (2012) and others have suggested that all 8 pairs should be tested in order to optimize a BiFC assay (Figure 10).

In addition, the failure of the co-precipitation assay to rule-out interaction between OCRL1 and the mutant ORP4 proteins (Fig. 8) suggests the possibility of non-specific signal contributing to the BiFC assay (Fig. 9). It is unclear whether the BiFC assay signal is a result of specific interaction between PPIs OCRL1 and ORP4L since the controls presented in the Western Blot analysis do not show the absence of interaction between OCRL1 and the mutants. Overall results of the three experiments show that there may or may not be specific interaction between the two proteins of interest in vitro.

The influence of orientation of the BiFC fusions on protein-protein interaction pairs has been observed previously in several studies **(**Bracha-Drori, Shichrur & Katz et al., 2004; Kerppola, 2008; Kerppola, Jackson & Sanders, 2009 and others). Kerppola, Jackson & Sanders (2009) note that although the protein pairs used in BiFC analysis of protein-protein interaction can be fused to the fluorescent protein fragments at either end, the exchange of fragments between different fusions will produce complexes that are not sterically equivalent.

There are 8 different fusion combinations (see Fig.10); so, it is reasonable that some complexes will be less flexible and or may experience steric hinderance.

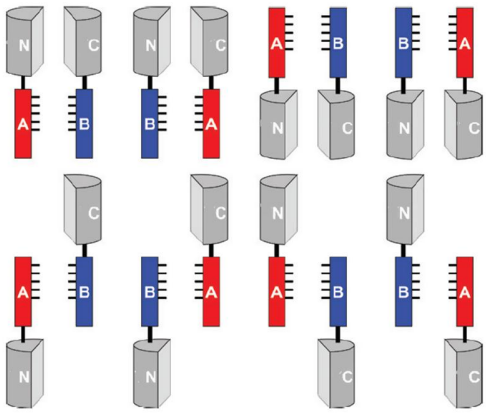

Figure 10. Multiple combinations of fusion proteins should be tested for BiFC. Amino- and carboxyl-terminal fusions can be used to test eight distinct combinations. The labels are the same as in Fig. 2. (chromophore in N tag not displayed). Adapted from (Kerppola, Jackson & Sanders, 2009).

In addition, in BiFC assays, steric hindrance can interfere with the reconstitution of the split protein by interfering with the refolding of the tertiary structure. The ability of the protein to refold will depend on the distance and orientation as well as approach angle of the split GFP N- and C-terminal regions (Wade, Méndez & Coussens et al., 2017). In addition, orientation can affect the efficiency of energy transfer. Proper experimental technique for optimization of BiFC assays should involve testing all 8 orientations and combinations of the fusions to the PPI pair (Kerppola, 2008; Kerppola, Jackson & Sanders, 2009; Wade, Méndez & Coussens et al., 2017). Wade, Méndez & Coussens et al. (2017) note that the linker (for instance a serine/glycine sequence) between the proteins of interest and the halves of the split reporter protein can play an important role in reducing steric hinderance and thus facilitate the reconstitution of the protein.

Visualization of OCRL1-ORP4L complex with BiFC

Protein-protein interactions (PPIs) are involved in many biological processes including transport, signal transduction. Szklarczyk, Franceschini & Wyder et al. (2014) point out that the concept of the protein network acknowledges the complex nature of the integration of functional interactions such as transient binding, formation of stable physical complexes, information relay, and others, and thus avoids the arbitrary partitioning of protein function into serial isolated mechanisms. Since their inception, PPI networks have been found in plants, yeast, worms, and humans (Yu, Braun & Yildirim et al., 2008; Venkatesan, Rual &Vazquez et al., 2008; Simonis, Rual & Carvunis et al., 2009; Lin, Zhou, & Shen et al., 2011; Kodama & Hu, 2012). Protein-protein interactions are the drivers of signal transduction in cells; therefore, it is crucial to investigate the molecular mechanisms involved in these processes.

Bimolecular fluorescence complementation (BiFC) assays have become a widely accepted methodology for identifying PPIs. The BiFC assay uses the complementation of two non-fluorescent fragments of a fluorescent protein (one C-terminal and one N-terminal fragment) that, when joined to two potentially interacting proteins, will restore the original intact fluorescent protein if the two partners do indeed interact (Fig. 11).

The first fluorescent complementation assay was carried out using Green Fluorescent Protein (GFP) (isolated from the *Aequorea victoria* jellyfish) in vitro in *E. coli* (Kodama& Hu, 2012). Two antiparallel zippers were affixed to the non-fluorescent, N-terminal and C-terminal fragments of GFP and the interaction was observed.

Following this initial success, a yellow fluorescent protein (EYFP)-based BiFC assay was carried out using a protein derived from GFP that allowed the fluorescence identification of protein interactions between the basic leucine zipper and proteins from the NF-kB protein family found in live mammalian cells (Kodama& Hu, 2012). Since 1994, a number of fluorescent proteins have been developed for BiFC assays which have unique physiochemical and spectral properties (Table 4).

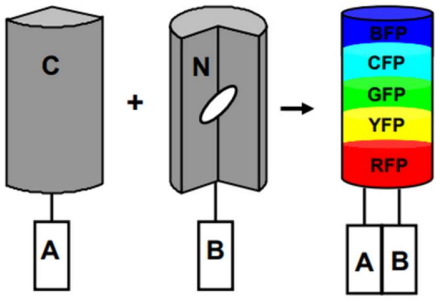

Figure 11. Principle of BiFC assay. Proteins A and B are fused to the C-terminal (C), and N-terminal fragments of a fluorescent protein. The interaction between proteins A and B brings two nonfluorescent fragments into proximity and reconstitutes an intact fluorescent protein, allowing direct visualization of the interaction in living cells. Various N- or C-terminal fragments from BFP, CFP, GFP, YFP, RFP and their variants have been demonstrated to support bimolecular fluorescence complementation (adapted from Shyu, Suarez & Liu et al., 2007).

Fluorescent protein	Excitation Peak (nm)[1]	Emission Peak (nm)[1]	Cell type or organism in the first use	Additional mutation
EBFP	382*	448*	Mammalian (COS-1)	None
Cerulean	439	479	Mammalian (COS-1)	None
ECFP	452	478	Mammalian (COS-1)	None
EGFP	488	512	Bacteria (*E. coli*)	None
GFP-S65T	489*	510	Plant (Onion epidermis)	V163A
frGFP	485*	510*	Bacteria (*E. coli*)	None
sfGFP	503*	518*	Mammalian (HeLa)	None
Dronpa	503*	518*	Mammalian (HEK293)	None
EYFP	514/515	527	Mammalian (COS-1)	None
Venus	515	528	Mammalian (COS-1)	None
Citrine	516	529	Mammalian (COS-1)	None
mRFP	549*	570*	Plant (Tobacco BY2 and Onion epidermis)	Q66T
DsRed monomer	556*	556*	Plant (Onion epidermis)	None
mCherry	587*	610*	Mammalian (Vero)	None
mKate	587*	621*	Mammalian (COS-7)	S158A

Table 4. The excitation and the emission spectra of BiFC systems. Asterisks (*) indicate that the spectra of the full-length fluorescent proteins were used when no measurement for the spectra of the reconstituted fluorescent protein was available. Excitation and emission spectra as shown at the Clontech website (http://www.clontech.com/) (Kodama & Hu, 2012).

Fluorescent proteins contain several helical structures along with b-strands which form a b-barrel inside of which an a-helix contains the chromophore (Kodama & Hu, 2012); they can be effectively split for BiFC analysis at a loop or within a β-stand (Fig. 12a, b) (Lai & Chiang, 2013). In the case of the GFP derivative, Venus (Figure 3), the fluorescent protein is 239 residues long and is usually split between the 7th and 8th b-sheet forming a N-terminal fragment (1-158) and a C-terminal fragment (159-239) (Lai & Chiang, 2013). The split at residue 155 causes the two non-fluorescent fragments to form opposing U-shaped structures which facilitate the reconstruction of the chromophore containing b-barrel when they come into close proximity (Fig. 12) (Isogai, Kawamoto & Inahata et al., 2011; Gookin & Assmann, 2014). The resulting reconstituted fluorescent protein can then be imaged using any fluorescence microscope (Fig. 12C).

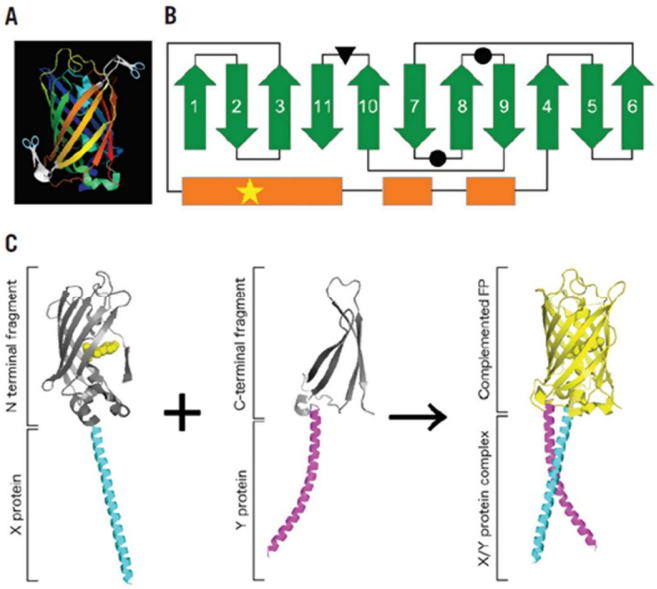

Figure 12. **Fluorescent proteins in BiFC assay.** (a) Three-dimensional structure of a fluorescent protein. The structure of the Venus yellow fluorescent protein. The structure of the Venus yellow fluorescent protein (PDB ID: 1MYW from RCSB Protein Data Bank) with the b-strands and a-helices visualized in rainbow colors using PyMol software. Two canonical split sites (between 7th and 8th b-strands, and between 8th and 9th b-strands) used for the BiFC assay are shown in white (and also indicated by scissors). (b) Folding topology of a fluorescent protein. The numbered green arrows and the orange boxes indicate b-strands and a-helices, respectively. The two closed circles indicate the positions of canonical split sites, and the arrowhead indicates the split site between the 10th and 11th b-strands. The star symbol indicates the fluorophore. (c) Principle of BiFC. The left structure represents the N-terminal BiFC fragment (VN155) fused to interacting protein X, with yellow indicating the fluorophore. The center structure represents the C-terminal BiFC fragment (VC155) fused to interacting protein Y. The a-helices of the bZIP domains of Jun (bJun) and Fos (bFos) are used as examples for the X and Y proteins respectively. The right structure shows the reconstituted fluorescent protein (FP) and the X/Y protein complex as ab Jun /bFos dimer). (Kodama & Hu, 2012).

Problems with the BiFC approach

Many researchers have pointed out that there are a large number of published studies of BiFC experiments where appropriate controls were not used to validate the signal present from split fused fluorescent proteins; this has left findings which indicate the detection of proximity or interactions between protein fragments of interest in a particular cellular location as detected through these flawed BiFC analyses inconclusive (Hiatt, Shyu, Duren & Hu, 2008; Kerppola, 2008; Kodama & Hu, 2012; Because fluorescent protein fragments are known to reconstitute to a certain extent in the absence of PPI interactions, random collision involving fluorescent fused protein fragments must be taken into consideration—particularly in BiFC experiments involving the overexpression of these protein fragments through transfection (Hiatt, Shyu, Duren & Hu, 2008; Kodama & Hu, 2012). In order to properly detect the signal generated by specific PPI, non-specific fluorescence signal in BiFC experiments must be identified and accounted for (Kodama & Hu, 2012).

The most stringent control a researcher can provide for a BiFC assay of PPI to ensure that random collision is not responsible for non-specific signal, is for one of the proteins from the suspected interaction pair to be altered such that just one of the interaction partners would harbor a single point mutation or a small deletion in the domain required for interaction with the unaltered partner to occur (Kudla & Bock, 2016). Finally, Kodama and Hu (2012) stress the importance of this type of control by pointing out that "In many cases, the fluorescent signal resulting from co-expression of the two non-fluorescent fragments not fused to interacting proteins is even stronger than that resulting from co-expression of the two fusion proteins (p. 293)." Because of this and other concerns, Kodama & Hu (2012) recommend the use of introducing a mutation to one member of the suspect PPI pair in order to eliminate the possibility that the observed signal is not non-specific.
Kudla & Bock, 2016). To date, many of the BiFC analyses in the literature involved transient overexpression of fusion proteins in cells, cultures, and tissues (Kudla & Bovk, 2016). Appropriate controls are crucial— especially to address the spontaneous reconstitution of the fluorescent protein giving rise to PPI signal that is not related to interaction between the protein fragments of interest (Kudla & Bock, 2016). Kodama and Hu (2012) point out that two non-interacting fluorescent protein fragments can come together in the same subcellular compartment as a result of random collision and their co-expression will, in turn, can generate fluorescence signal; signal generated from such random collisions is considered to be "non-specific".

Because BiFC assays measure proximity of interacting proteins, reconstitution of the fluorescent protein does not necessarily signify that the protein fragment pair of interest is indeed interacting.

Advantages of the BiFC approach over other complementation methods

The BiFC approach has several advantages over other complementation methods. Firstly, the detection of protein-protein interaction is facilitated by the strength of the fluorescence from the assembled complex which allows for direct visualization of the interaction of fusion proteins in subcellular locations within the cellular environment without the addition of fluorogenic or chromogenic imaging agents. Such agents may interact with the proteins of interest. In addition, chromogenic or fluorogenic substrates or ligands are not always evenly

distributed (Kerppola, 2008). Furthermore, the method can be used for many types of proteins and does not require a priori knowledge about the protein structures or the structures or identities of potential interaction partners (Kerppola, 2008; Pratt, Owens & Hockerman et al., 2016).

Because the fluorescence signal is derived directly from the reassembled fluorescent protein, detection is possible even when the mole fraction of formed complex between the fusion proteins is low. In addition, signal can be detected with low levels of protein expression (Kerppola, 2008). The N-terminus and C-terminus of the GFP-derivative, Venus, abbreviated VN, and VC, respectively, are currently in wide use for the BiFC analysis of mammalian cells. The popularity of the Venus fluorescent protein for assay studies is based on its lower sensitivity to environmental factors relative to earlier proteins such as GFP (Pratt, Owens & Hockerman et al., 2016). We chose to use VC and VN cloning vectors in our study of the interactions of OCRL1 with ORP4L.

ACKNOWLEDGEMENTS

This work was carried out at Vesa Olkkonen's research lab at Minerva Foundation Institute for Medical Research. I am profoundly grateful to my supervisor Professor Dr.Vesa Olkkonen for giving me the opportunity to work for him in his research project. I would also like to thank my co-supervisor Dr. Marion Weber-Boyvat for her guiding me through this period with her knowledge and expertise.

I would also like to thank all my lab members and my Professors and administration heads at Faculty of Biological and Environmental sciences.

My research would not have been possible without the aid and support from The Sigrid Jusélius Foundation and Academy of Finland, hence my heartfelt thanks to them.

Finally, special thanks to my mother Mrs. Jaya shah for supporting me throughout this journey.

References

Beh, C., McMaster, C., Kozminski, K., & Menon, A. (2012). A detour for yeast oxysterol binding proteins. *Journal of Biological Chemistry*, *287*(14), 11481-11488. doi: 10.1074/jbc.r111.338400.

Bjorkhem, I., & Diczfalusy, U. (2002). Oxysterols: Friends, foes, or just fellow passengers? *Arteriosclerosis, Thrombosis, and Vascular Biology*, *22*(5), 734-742. doi: 10.1161/01.atv.0000013312.32196.49.

Bracha-Drori, K., Shichrur, K., Katz, A., Oliva, M., Angelovici, R., Yalovsky, S., & Ohad, N. (2004). Detection of protein-protein interactions in plants using bimolecular fluorescence complementation. *The Plant Journal*, *40*(3), 419-427. doi: 10.1111/j.1365-313x.2004.02206.x

Burgett, A., Poulsen, T., Wangkanont, K., Anderson, D., Kikuchi, C., & Shimada, K. et al. (2011). Natural products reveal cancer cell dependence on oxysterol-binding proteins. *Nature Chemical Biology*, *7*(9), 639-647. doi: 10.1038/nchembio.625.

Charman, M., Colbourne, T., Pietrangelo, A., Kreplak, L., & Ridgway, N. (2014). Oxysterol-binding protein (OSBP)-related protein 4 (ORP4) is essential for cell proliferation and survival. *Journal of Biological Chemistry*, *289*(22), 15705-15717. doi: 10.1074/jbc.m114.571216.

Chiapparino, A., Maeda, K., Turei, D., Saez-Rodriguez, J., & Gavin, A. (2016). The orchestra of lipid-transfer proteins at the crossroads between metabolism and signaling. *Progress in Lipid Research*, *61*, 30-39. doi: 10.1016/j.plipres.2015.10.004.

Chung, J., Torta, F., Masai, K., Lucast, L., Czapla, H., & Tanner, L. et al. (2015). PI4P/phosphatidylserine countertransport at ORP5- and ORP8-mediated ER-plasma membrane contacts. *Science*, *349*(6246), 428-432. doi: 10.1126/science.aab1370.

Dawson, P., Ridgway, N., Slaughter, C., Brown, M., & Goldstein, J. (1989). cDNA Cloning and Expression of Oxysterol-binding Protein, an Oligomer with a Potential Leucine Zipper. *Journal Of Biological Chemistry*, *264*(28), 16798-1680.

Di Paolo, G., & De Camilli, P. (2006). Phosphoinositides in cell regulation and membrane dynamics. *Nature*, *443*(7112), 651-657. doi: 10.1038/nature05185.

Fahy, E., Subramaniam, S., Murphy, R., Nishijima, M., Raetz, C., & Shimizu, T. et al. (2008). Update of the LIPID MAPS comprehensive classification system for lipids. *Journal Of Lipid Research*, *50*(Supplement), S9-S14. doi: 10.1194/jlr.r800095-jlr200

Ferguson, K., Kavran, J., Sankaran, V., Fournier, E., Isakoff, S., Skolnik, E., & Lemmon, M. (2000). Structural basis for discrimination of 3-phosphoinositides by Pleckstrin homology domains. *Molecular Cell*, *6*(2), 373-384. doi: 10.1016/s1097-2765(00)00037-x.

Fournier, M., Guimarães da Costa, F., Paschoal, M., Ronco, L., Carvalho, M., Pardee, A. (1999). Identification of a gene encoding a human oxysterol-binding protein-homologue: a potential general molecular marker for blood dissemination of solid tumors. *Cancer Res.*, *59*(15): 3748-53. PMID: 10446991.

Henriques Silva, N., Vasconcellos Fournier, M., Pimenta, G., Pulcheri, W., Spector, N., da Costa Carvalho, M. (2003). HLM/OSBP2 is expressed in chronic myeloid leukemia. *Int J Mol Med*. *12*(4):663-6. PMID: 12964051

Gillooly, D., Simonsen, A., & Stenmark, H. (2001). Cellular functions of phosphatidylinositol 3-phosphate and FYVE domain proteins. *Biochemical Journal*, *355*(2), 249. doi: 10.1042/0264-6021:3550249.

Gookin, T., & Assmann, S. (2014). Significant reduction of BiFC non-specific assembly facilitatesin plantaassessment of heterotrimeric G-protein interactors. *The Plant Journal*, *80*(3), 553-567. doi: 10.1111/tpj.12639

Grainger, D., Tavelis, C., Ryan, A., & Hinchliffe, K. (2012). The emerging role of PtdIns5P: another signalling phosphoinositide takes its place. *Biochemical Society Transactions*, *40*(1), 257-261. doi: 10.1042/bst20110617.

Hiatt, S., Shyu, Y., Duren, H., & Hu, C. (2008). Bimolecular fluorescence complementation (BiFC) analysis of protein interactions in Caenorhabditis elegans. *Methods*, *45*(3), 185-191. doi: 10.1016/j.ymeth.2008.06.003

Hong, N., Qi, A., & Weaver, A. (2015). PI(3,5)P2 controls endosomal branched actin dynamics by regulating cortactin–actin interactions. *Journal of Cell Biology*, *210*(5), 753-769. doi: 10.1085/jgp.1463oia50.

Im, Y., Raychaudhuri, S., Prinz, W., & Hurley, J. (2005). Structural mechanism for sterol sensing and transport by OSBP-related proteins. *Nature*, *437*(7055), 154-158. doi: 10.1038/nature03923.

Isogai, M., Kawamoto, Y., Inahata, K., Fukada, H., Sugimoto, K., & Tada, T. (2011). Structure and characteristics of reassembled fluorescent protein, a new insight into the reassembly mechanisms. *Bioorganic & Medicinal Chemistry Letters*, *21*(10), 3021-3024. doi: 10.1016/j.bmcl.2011.03.039

Kaiser, S., Brickner, J., Reilein, A., Fenn, T., Walter, P., & Brunger, A. (2005). Structural basis of FFAT motif-mediated ER targeting. *Structure*, *13*(7), 1035-1045. doi: 10.1016/j.str.2005.04.010. Kerppola, T. (2006). Design and implementation of bimolecular fluorescence complementation (BiFC) assays for the visualization of protein interactions in living cells. *Nature Protocols*, *1*(3), 1278-1286. doi: 10.1038/nprot.2006.201

Kerppola, T. (2008). Bimolecular Fluorescence Complementation (BiFC) Analysis as a Probe of Protein Interactions in Living Cells. *Annual Review Of Biophysics*, *37*(1), 465-487. doi: 10.1146/annurev.biophys.37.032807.125842

Kerppola, T., Jackson (ed), S., & Sanders (ed), J. (2009). Reviewing the latest developments in the science of green fluorescent protein. *Chemical Society Reviews*, *38*(10), 2875-2886.

Kim, Y., Guzman-Hernandez, M., & Balla, T. (2011). A highly dynamic ER-derived phosphatidylinositol-synthesizing organelle supplies phosphoinositides to cellular membranes. *Developmental Cell*, *21*(5), 813-824. doi: 10.1016/j.devcel.2011.09.005.

Kodama, Y., & Hu, C. (2012). Bimolecular fluorescence complementation (BiFC): A 5-year update and future perspectives. *Biotechniques*, *53*(5). doi: 10.2144/000113943

Kudla, J., & Bock, R. (2016). Lighting the Way to Protein-Protein Interactions: Recommendations on Best Practices for Bimolecular Fluorescence Complementation Analyses. *The Plant Cell*, *28*(5), 1002-1008. doi: 10.1105/tpc.16.00043

Lai, H., & Chiang, C. (2013). Bimolecular Fluorescence Complementation (BiFC) Assay for Direct Visualization of Protein-Protein Interaction in vivo. *BIO-PROTOCOL*, *3*(20). doi: 10.21769/bioprotoc.935

Lehto, M., Chinetti, H., Johansson, M., Ehnholm, C., Staels, B., Ikonen, E., & Olkkonen, V. (2001). The OSBP-related protein family in humans. *Journal of Lipid Research*, *42*(8), 1203-1213.

Lev, S. (2010). Non-vesicular lipid transport by lipid-transfer proteins and beyond. *Nature Reviews Molecular Cell Biology*, *11*(10), 739-750. doi: 10.1038/nrm2971.

Li, J., Xiao, Y., Lai, C., Lou, N., Ma, H., & Zhu, B. et al. (2016). Oxysterol-binding protein-related protein 4L promotes cell proliferation by sustaining intracellular Ca2+ homeostasis in cervical carcinoma cell lines. *Oncotarget*, *7*(40). doi: 10.18632/oncotarget.11671.

Lin, M., Zhou, X., Shen, X., Mao, C., & Chen, X. (2011). The Predicted Arabidopsis Interactome Resource and Network Topology-Based Systems Biology Analyses. *The Plant Cell*, *23*(3), 911-922. doi: 10.1105/tpc.110.082529

Loewen, C. J.R., Roy, A. Levine, T. P. (2003). A conserved ER targeting motif in three families of lipid binding proteins and in Opi1p binds VAP. *The EMBO Journal*, *22*(9), 2025-2035. doi: 10.1093/emboj/cdg201.

Lowe, M. (2005). Structure and function of the Lowe syndrome protein OCRL1. *Traffic*, *6*(9), 711-719. doi: 10.1111/j.1600-0854.2005.00311.x.

Mesmin, B., Bigay, J., Moser von Filseck, J., Lacas-Gervais, S., Drin, G., & Antonny, B. (2013). A four-step cycle driven by PI(4)P hydrolysis directs sterol/PI(4)P exchange by the ER-Golgi tether OSBP. *Cell*, *155*(4), 830-843. doi: 10.1016/j.cell.2013.09.056.golgi.

Mosavi, L., Cammett, T., Desrosiers, D., & Peng, Z. (2004). The ankyrin repeat as molecular architecture for protein recognition. *Protein Science*, *13*(6), 1435-1448. doi: 10.1110/ps.03554604.

Moser von Filseck, J., opi, A., Delfosse, V., Vanni, S., Jackson, C., Bourguet, W., & Drin, G. (2015). Phosphatidylserine transport by ORP/Osh proteins is driven by phosphatidylinositol 4-phosphate. *Science*, *349*(6246), 432-436. doi: 10.1126/science.aab1346.

Ngo, M., Colbourne, T., & Ridgway, N. (2010). Functional implications of sterol transport by the oxysterol-binding protein gene family. *Biochemical Journal*, *429*(1), 13-24. doi: 10.1042/bj20100263.

Olkkonen, V., & Li, S. (2013). Oxysterol-binding proteins: Sterol and phosphoinositide sensors coordinating transport, signaling and metabolism. *Progress in Lipid Research*, *52*(4), 529-538. doi: 10.1016/j.plipres.2013.06.004.

Overview of the Immunoprecipitation (IP) Technique | Thermo Fisher Scientific. (2018). Retrieved from https://www.thermofisher.com/ca/en/home/life-science/protein-biology/protein-biology-learning-center/protein-biology-resource-library/pierce-protein-methods/immunoprecipitation-ip.html

Park, I., Ndjomou, J., Wen, Y., Liu, Z., Ridgway, N., Kao, C., & He, J. (2013). Inhibition of HCV replication by oxysterol-binding protein-related protein 4 (ORP4) through interaction with HCV NS5B and alteration of lipid droplet formation. *Plos ONE*, *8*(9), e75648. doi: 10.1371/journal.pone.0075648.

Pirruccello, M., & De Camilli, P. (2012). Inositol 5-phosphatases: insights from the Lowe syndrome protein OCRL. *Trends in Biochemical Sciences*, *37*(4), 134-143. doi: 10.1016/j.tibs.2012.01.002.

Pratt, E., Owens, J., Hockerman, G., & Hu, C. (2016). Bimolecular Fluorescence Complementation (BiFC) Analysis of Protein–Protein Interactions and Assessment of Subcellular Localization in Live Cells. *Methods In Molecular Biology*, 153-170. doi: 10.1007/978-1-4939-6352-2_9

Protein Gel Staining Methods | Thermo Fisher Scientific. (2018). Retrieved from https://www.thermofisher.com/ca/en/home/life-science/protein-biology/protein-biology-learning-center/protein-biology-resource-library/pierce-protein-methods/protein-gel-stains.html

Raychaudhuri, S., & Prinz, W. (2010). The diverse functions of oxysterol-binding proteins. *Annual Review of Cell and Developmental Biology*, *26*(1), 157-177. doi: 10.1146/annurev.cellbio.042308.113334.

Raychaudhuri, S., Im, Y., Hurley, J., & Prinz, W. (2006). Nonvesicular sterol movement from plasma membrane to ER requires oxysterol-binding protein–related proteins and phosphoinositides. *The Journal of Cell Biology*, *173*(1), 107-119. doi: 10.1083/jcb.200510084.

Rocha, N., Kuijl, C., van der Kant, R., Janssen, L., Houben, D., & Janssen, H. et al. (2009). Cholesterol sensor ORP1L contacts the ER protein VAP to control Rab7–RILP–p150 glued and late endosome positioning. *The Journal of Cell Biology*, *185*(7), 1209-1225. doi: 10.1083/jcb.200811005.

Schmid, A., Wise, H., Mitchell, C., Nussbaum, R., & Woscholski, R. (2004). Type II phosphoinositide 5-phosphatases have unique sensitivities towards fatty acid composition and head group phosphorylation. *FEBS Letters*, *576*(1-2), 9-13. doi: 10.1016/j.febslet.2004.08.052.

Schulz, T., Choi, M., Raychaudhuri, S., Mears, J., Ghirlando, R., Hinshaw, J., & Prinz, W. (2009). Lipid-regulated sterol transfer between closely apposed membranes by oxysterol-binding protein homologues. *The Journal of Cell Biology*, *187*(6), 889-903. doi: 10.1083/jcb.200905007.

Shyu, Y., Suarez, C., Liu, H., Deng, X., & Hu, C. (2007). Bimolecular Fluorescence complementation (BiFC) and beyond. *Microscopy And Microanalysis*, *13*(S02). doi: 10.1017/s1431927607073783

Simonis, N., Rual, J.-F., Carvunis, A.-R., Tasan, M., Lemmens, I., Hirozane-Kishikawa, T., … Vidal, M. (2009). Empirically-controlled mapping of the *Caenorhabditis elegans* protein-protein interactome network. *Nature Methods*, *6*(1), 47–54.

Staiano, L., De Leo, M., Persico, M., & De Matteis, M. (2015). Mendelian disorders of PI metabolizing enzymes. *Biochimica et Biophysica Acta (BBA) - Molecular and Cell Biology of Lipids*, *1851*(6), 867-881. doi: 10.1016/j.bbalip.2014.12.001.

Stefan, C., Manford, A., Baird, D., Yamada-Hanff, J., Mao, Y., & Emr, S. (2011). Osh proteins regulate phosphoinositide metabolism at ER-plasma membrane contact sites. *Cell*, *144*(3), 389-401. doi: 10.1016/j.cell.2010.12.034.

Szklarczyk, D., Franceschini, A., Wyder, S., Forslund, K., Heller, D., & Huerta-Cepas, J. et al. (2014). STRING v10: protein–protein interaction networks, integrated over the tree of life. *Nucleic Acids Research*, *43*(D1), D447-D452. doi: 10.1093/nar/gku1003

Taylor, F., Saucier, S., Shown, E., Parish, E., & Kandutsch, A. (1984). Correlation between oxysterol binding to a cytosolic binding protein and potency in the repression of hydroxymethylglutaryl coenzyme A reductase. *The Journal of Biological Chemistry*, *259*(20), 1282-1287.

Tong, J., Manik, M., Yang, H., & Im, Y. (2016). Structural insights into nonvesicular lipid transport by the oxysterol binding protein homologue family. *Biochimica et Biophysica Acta (BBA) - Molecular and Cell Biology Of Lipids*, *1861*(8), 928-939. doi: 10.1016/j.bbalip.2016.01.008.

Tong, J., Yang, H., Yang, H., Eom, S., & Im, Y. (2013). Structure of Osh3 reveals a conserved mode of phosphoinositide binding in oxysterol-binding proteins. *Structure*, *21*(7), 1203-1213. doi: 10.1016/j.str.2013.05.007.

Umate, P. (2011). Oxysterol binding proteins (OSBPs) and their encoding genes in arabidopsis and rice. *Steroids*, *76*(5), 524-529. doi: 10.1016/j.steroids.2011.01.007.

Ungewickell, A., Ward, M., Ungewickell, E., & Majerus, P. (2004). The inositol polyphosphate 5-phosphatase Ocrl associates with endosomes that are partially coated with clathrin. *Proceedings of The National Academy of Sciences*, *101*(37), 13501-13506. doi: 10.1073/pnas.0405664101.

Venditti, R., Masone, M., Wilson, C., & De Matteis, M. (2016). PI(4)P homeostasis: Who controls the controllers?. *Advances in Biological Regulation*, *60*, 105-114. doi: 10.1016/j.jbior.2015.09.007.

Venkatesan, K., Rual, J., Vazquez, A., Stelzl, U., Lemmens, I., & Hirozane-Kishikawa, T. et al. (2008). An empirical framework for binary interactome mapping. *Nature Methods*, *6*(1), 83-90. doi: 10.1038/nmeth.1280

Wade M, Méndez J, Coussens NP, et al. Inhibition of Protein-Protein Interactions: Cell-Based Assays. 2017 Nov 20. In: Sittampalam GS, Coussens NP, Brimacombe K, et al., editors. Assay Guidance Manual [Internet]. Bethesda (MD): Eli Lilly & Company and the National

Wijdeven, R., Janssen, H., Nahidiazar, L., Janssen, L., Jalink, K., Berlin, I., & Neefjes, J. (2016). Cholesterol and ORP1L-mediated ER contact sites control autophagosome transport and fusion with the endocytic pathway. *Nature Communications*, *7*, 11808. doi: 10.1038/ncomms11808.

Wyles, J., Perry, R., & Ridgway, N. (2007). Characterization of the sterol-binding domain of oxysterol-binding protein (OSBP)-related protein 4 reveals a novel role in vimentin organization. *Experimental Cell Research*, *313*(7), 1426-1437. doi: 10.1016/j.yexcr.2007.01.018.

Yu, H., Braun, P., Yildirim, M., Lemmens, I., Venkatesan, K., & Sahalie, J. et al. (2008). High-Quality Binary Protein Interaction Map of the Yeast Interactome Network. *Science*, *322*(5898), 104-110. doi: 10.1126/science.1158684

Zhong, W., Yi, Q., Xu, B., Li, S., Wang, T., & Liu, F. et al. (2016). ORP4L is essential for T-cell acute lymphoblastic leukemia cell survival. *Nature Communications*, *7*, 12702. doi: 10.1038/ncomms12702.